Stimulator of interferon genes (STING) is an essential proviral host factor for human rhinovirus species A and C

Kevin L. McKnight[a,1], Karen V. Swanson[b,1], Kathryn Austgen[c,1], Cindy Richards[c,1], Jonathan K. Mitchell[a], David R. McGivern[b], Ethan Fritch[d], John Johnson[c], Katja Remlinger[c], Michal Magid-Slav[c], Maryna Kapustina[e], Shihyun You[c,2], and Stanley M. Lemon[a,b,d,2]

[a]Lineberger Comprehensive Cancer Center, The University of North Carolina at Chapel Hill, Chapel Hill, NC 27599; [b]Division of Infectious Diseases, Department of Medicine, The University of North Carolina at Chapel Hill, Chapel Hill, NC 27599; [c]Research & Development, GlaxoSmithKline, Collegeville, PA 19426; [d]Department of Microbiology and Immunology, The University of North Carolina at Chapel Hill, Chapel Hill, NC 27599; and [e]Department of Cell Biology and Physiology, The University of North Carolina at Chapel Hill, Chapel Hill, NC 27599

Edited by Peter Sarnow, Stanford University School of Medicine, Stanford, CA, and approved September 4, 2020 (received for review July 20, 2020)

Human rhinoviruses (RVs) are positive-strand RNA viruses that cause respiratory tract disease in children and adults. Here we show that the innate immune signaling protein STING is required for efficient replication of members of two distinct RV species, RV-A and RV-C. The host factor activity of STING was identified in a genome-wide RNA interference (RNAi) screen and confirmed in primary human small airway epithelial cells. Replication of RV-A serotypes was strictly dependent on STING, whereas RV-B serotypes were notably less dependent. Subgenomic RV-A and RV-C RNA replicons failed to amplify in the absence of STING, revealing it to be required for a step in RNA replication. STING was expressed on phosphatidylinositol 4-phosphate (PI4P)-enriched membranes and was enriched in RV-A16 compared with RV-B14 replication organelles isolated in isopycnic gradients. The host factor activity of STING was species-specific, as murine STING (mSTING) did not rescue RV-A16 replication in STING-deficient cells. This species specificity mapped primarily to the cytoplasmic, ligand-binding domain of STING. Mouse-adaptive mutations in the RV-A16 2C protein allowed for robust replication in cells expressing mSTING, suggesting a role for 2C in recruiting STING to RV-A replication organelles. Palmitoylation of STING was not required for RV-A16 replication, nor was the C-terminal tail of STING that mediates IRF3 signaling. Despite co-opting STING to promote its replication, interferon signaling in response to STING agonists remained intact in RV-A16 infected cells. These data demonstrate a surprising requirement for a key host mediator of innate immunity to DNA viruses in the life cycle of a small pathogenic RNA virus.

innate immunity | cGAS | phosphatidylinositol 4-phosphate | replication organelle | host range

Human rhinoviruses (RVs) are ubiquitous respiratory pathogens composing a large group of antigenically diverse, positive-strand RNA viruses classified within the *Enterovirus* genus of the *Picornaviridae* family (1, 2). The most frequent cause of the common cold, RV infections among the young are associated with the development of asthma (3, 4). In older individuals, RV infections may also lead to acute exacerbations of asthma and chronic obstructive pulmonary disease and are a significant cause of lower respiratory tract disease (5, 6). RVs are grouped phylogenetically into three species, each containing multiple serotypes (2, 7). Unlike RV-A and RV-B, which have been recognized for decades and readily propagated in conventional cell cultures, RV-C was identified more recently and replicates in vitro only in cells engineered to express a critical entry factor, cadherin-related family member 3 (CDHR3) (8). RV-C is strongly associated with severe respiratory tract infections in young children and is more closely related to RV-A than to RV-B (2, 7, 9, 10). Nearly all hospital visits related to RV-triggered asthma are due to infections with RV-A or RV-C viruses, with RV-C associated with more severe symptoms (10–12).

The molecular mechanisms underlying replication of these RNA viruses are only partially understood. Enteroviral RNAs are synthesized on the cytosolic surface of membranous cytoplasmic tubulovesicular structures (13–15). These replication organelles are derived from remodeled endoplasmic reticulum (ER) or Golgi membranes and contain multiple viral nonstructural proteins, including 2B, 2C, and an RNA-dependent RNA polymerase, $3D^{pol}$ (16). The formation of replication organelles is associated with a striking reordering of cellular lipid metabolism, with phosphatidylinositol 4-kinase-IIIβ (PI4Kβ) playing a key role. PI4Kβ is recruited to membranes at the site of replication by the viral 3A protein acting in concert with host acyl-CoA binding domain-containing 3 (ACBD3) (13, 17, 18). PI4Kβ mediates the enrichment of these membranes with phosphatidylinositol 4-phosphate (PI4P), leading to subsequent recruitment of oxysterol-binding protein 1 (OSBP1), which enhances cholesterol flux into the membranes (18). Thus, ACBD3, PI4Kβ, and OSBP1 are all crucial host factors for RV replication.

Significance

We show here that efficient replication of RV-A and RV-C viruses, common respiratory pathogens with positive-strand RNA genomes, requires STING, a host protein with canonical function in innate immune responses to DNA viruses. STING is enriched in PI4P-containing membranes of RV-A replication organelles and is essential for a step in replication of the viral RNA genome. Its host factor activity is highly species-specific, and adaptation of the RV-16 virus to murine STING promotes RV-16 replication in cells of murine origin. These findings add substantially to the current understanding of essential host factors that restrict the host species range of RVs and limit the development of small animal models.

Author contributions: K.L.M., K.V.S., K.A., C.R., J.K.M., M.K., S.Y., and S.M.L. designed research; K.L.M., K.V.S., K.A., C.R., J.K.M., D.R.M., E.F., J.J., K.R., M.M.-S., M.K., and S.Y. performed research; K.L.M., K.V.S., K.A., C.R., J.K.M., K.R., M.K., S.Y., and S.M.L. analyzed data; and K.L.M., K.V.S., M.K., S.Y., and S.M.L. wrote the paper.

Competing interest statement: K.A., C.R., J.J., K.R., M.M.-S., and S.Y. are currently or were previously employees of GlaxoSmithKline.

This article is a PNAS Direct Submission.

[1]K.L.M., K.V.S., K.A., and C.R. contributed equally to this work.

[2]To whom correspondence may be addressed. Email: shihyun.k.you@gsk.com or smlemon@med.unc.edu.

This article contains supporting information online at https://www.pnas.org/lookup/suppl/doi:10.1073/pnas.2014940117/-/DCSupplemental.

First published October 15, 2020.

The intracellular replication of poliovirus, a closely-related enterovirus, is also dependent on components of host autophagic signaling, including LC3 protein that associates with the membranes of replication organelles in a nonlipidated form (19, 20). Whether this is also true for rhinoviruses is uncertain. Unlike poliovirus, RV-A1a replication is not influenced by chemical compounds that promote or inhibit autophagy, rapamycin, and 3-methyadenine (3-MA) respectively, while similar studies of RV-A2 produced conflicting results (21, 22). These latter data show that even among closely related viruses in the same picornaviral genus, host factors involved in remodeling membranes and generating replication organelles may vary substantially. Here we describe a surprising requirement for the Stimulator of Interferon Genes (STING) protein in intracellular replication of RV-A and RV-C viruses. STING (also known as MITA, ERIS, or MPYS) is an essential adaptor protein downstream of cGMP-AMP synthase (cGAS) in the innate immune cytosolic DNA-sensing pathway, and thus is typically associated with antiviral rather than proviral effects (23–27). We show that RV-A16 replication organelles are enriched in STING, and that transfected subgenomic RV-A16 and RV-C15 RNA replicons fail to amplify in the absence of STING. Genetic evidence links STING to the nonstructural 2C protein of RV-A, which is known to play a crucial role in the formation of replication organelles.

Results

Genome-Wide Screen Identifies STING as an RV-A2 Host Factor. STING was identified as a host protein required for RV-A2 replication in a genome-wide siRNA screen targeting 22,909 genes in HeLa-Ohio cells (Fig. 1 *A* and *B* and *SI Appendix*, Fig. S1*B*). Of 1,750 potential "hits," subsequent analyses identified a total of 125 candidate genes for which on-target knockdown with two or more of four individual siRNAs protected cells against RV-A2's cytopathic effect (CPE) (*SI Appendix*, Fig. S1*B*). *STING1 (*formerly *TMEM173*), which encodes the innate immune signaling adapter protein STING, was prominent among these candidate host factors. Single siRNAs targeting *STING1* passed the "C911" test for target sequence specificity (28); modified siRNAs in which bases 9 to 11 were swapped with their complement did not protect against RV-A2 CPE (Fig. 1*C*). *STING1*-specific siRNAs provided robust protection against a second RV-A serotype, RV-A16, in HeLa-Ohio cells, but not against coxsackievirus B3 (CV-B3), another enterovirus, or respiratory syncytial virus (RSV), an unrelated respiratory tract pathogen (Fig. 1*D*). Importantly, we confirmed that RNA interference (RNAi)-mediated STING depletion had strong antiviral effects against RV-A16 in primary human small airway epithelial cells (SAECs), reducing both the abundance of RV-A16 RNA and the proportion of cells containing detectable viral antigen (Fig. 1 *E* and *F*).

STING Promotes RV-A and RV-C Genome Amplification. That human rhinoviruses should require STING for infection is surprising, as STING is an important antiviral signaling protein that promotes interferon (IFN) synthesis in cells infected with DNA viruses (24, 29). The basal expression of STING is very low in Huh-7 cells, which are derived from a human hepatocellular carcinoma (Fig. 2*A* and *SI Appendix*, Fig. S2*A*). Accordingly, Huh-7 cells were nonpermissive for RV-A16 infection unless transfected with plasmid DNA expressing STING (Fig. 2*B*). Because transfected cytosolic DNA might induce STING signaling, we established stably transduced Huh-7 cells in which HA-tagged human STING (hSTING-HA) is expressed under control of the inducible tetracycline (Tet-On) promoter (Huh-7/hSTING cells) (Fig. 2*C* and *SI Appendix*, Fig. S2*B*). Flow cytometry documented the presence of viral double-stranded RNA (dsRNA) replication intermediates as early as 6 h after RV-A16 infection of Huh-7/hSTING cells induced to express STING in the presence of doxycycline (+Dox), or transfection of induced cells with synthetic RV-A16 RNA (Fig. 2 *C* and *D* and *SI Appendix*, Fig. S3 *A* and *B*). In contrast, minimal or no dsRNA intermediates were produced in the absence of doxycycline (−Dox). Collectively, these results show that STING facilitates the RV-A lifecycle.

To define the step within the RV lifecycle that requires STING, Huh-7/hSTING cells were electroporated with RV-A species genomic RNAs. RV-A16 and RV-A1a genome-length RNAs produced abundant dsRNA in cells induced to express STING (+Dox), but not in STING-deficient cells (-Dox) (Fig. 2*E*). Pleconaril, an antiviral compound that binds the RV capsid and prevents cell entry (30), had no effect on STING-dependent dsRNA or VP2 capsid protein expression at 6 or 24 h but strongly inhibited subsequent increases at 48 and 72 h (*SI Appendix*, Fig. S3 *A* and *B*). This indicates that STING is required for second-round infections of naïve cells that are sensitive to pleconaril inhibition. dsRNA was detected in a small proportion of noninduced cells electroporated with RV-A1a RNA (Fig. 2*E*), most likely reflecting low-level, leaky expression of Tet-regulated STING-HA.

As there was no evidence of RV-A16 replication in noninduced cells, different RV-A serotypes may vary somewhat in their requirement for STING. Surprisingly, however, a much greater difference was observed with RV-B14 RNA, which replicated robustly without STING induction (Fig. 2*E*). This led us to explore in greater detail the requirement for STING among different RV species. In addition to the STING dependence of RV-A1a, -A2, and -A16 described above, we found that the production of dsRNA replication intermediates by 12 other RV-A serotypes (RV-A1b, A11, A24, A28, A50, A53, A56, A61, A65, A94, A95, A100) was highly dependent on ectopically expressed STING in Huh7scr cells inoculated with cell-free virus (*SI Appendix*, Fig. S4 *A* and *B*). Compared with empty vector, transfecting Huh7scr cells with a STING expression vector increased the percentage of cells containing detectable dsRNA by a median of 84.2-fold (range, 10.9- to 197-fold) (*SI Appendix*, Fig. S4*C*). Similar experiments could not be done with seven different RV-B serotypes (RV-B4, B6, B14, B48, B52, B84, B93) because each induced robust CPEs in cells transfected only with empty vector. Thus, although we have tested only a small fraction of all RV-A and RV-B serotypes, RV-A rhinoviruses appear to be more dependent on STING for replication compared with RV-B species rhinoviruses. Replication of the closely related respiratory enterovirus EV-D68 (once classified among the rhinoviruses) was not dependent on STING (*SI Appendix*, Fig. S5 *A* and *B*).

To further identify the step in RV-A replication that requires STING, we transfected Huh-7/hSTING cells with an RV-A16 replicon RNA in which sequence-encoding luciferase replaces the P1 capsid-coding region of the RV genome (Fig. 2 *F*, *Top*). This RNA replicates autonomously in permissive cells, recapitulating viral polyprotein translation and RNA synthesis, but bypasses steps in the viral life cycle involving cell entry, uncoating, assembly, and egress. Thus, luciferase expressed by this replicon is a measure of RV-A16 polyprotein translation and replicon RNA synthesis. Consistent with the requirement of STING for either of these steps in the viral replication cycle, luciferase expression was enhanced by induction (+Dox) of STING in transfected Huh-7/hSTING cells (Fig. 2 *F*, *Bottom Left*). Luciferase expression from similar RV-A1a and RV-C15 replicons was also enhanced by STING expression, but that from an RV-B14 replicon was not (Fig. 2 *F*, *Bottom Right*). This latter observation is consistent with the robust replication of RV-B14 virus in the absence of STING induction noted above (Fig. 2*E*). Importantly, the presence or absence of STING did not influence the expression of luciferase from replication-incompetent replicon RNAs with lethal mutations in the $3D^{pol}$ RNA-dependent RNA polymerase (Fig. 2 *F*, *Bottom Right*). Luciferase expressed by these RNAs is a measure only of viral translation mediated by the

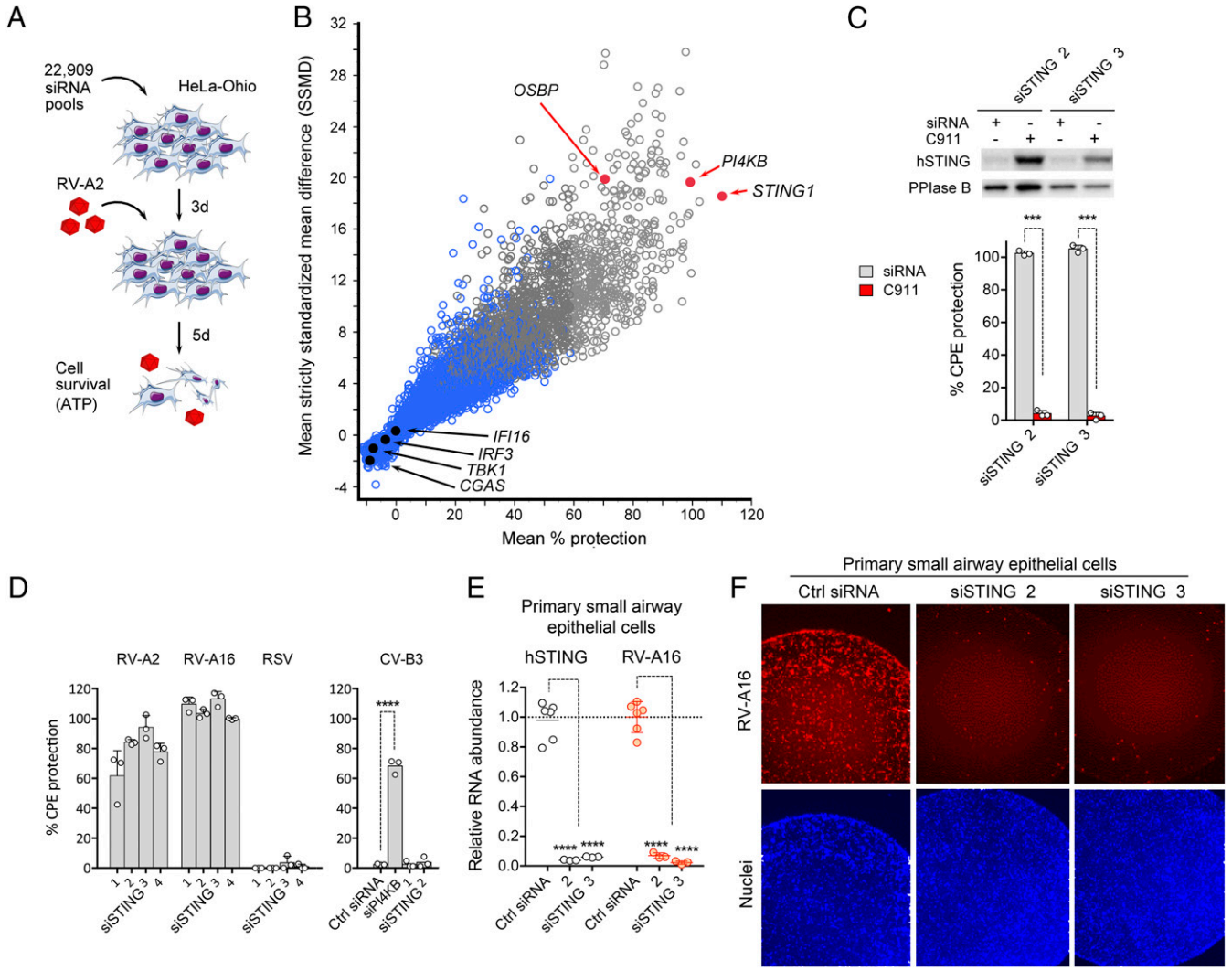

Fig. 1. RNAi-based screen for essential RV-A2 host factors. (*A*) Experimental design. (*B*) Results of the primary screen with mean effect size (strictly standardized mean difference [SSMD]) vs. mean percent protection from CPE for pools of four siRNAs targeting 22,909 human genes in four to six replicate assays. Hits (blue or red symbols) were defined as siRNA pools providing ≥14% mean protection with mean SSMD ≥5 in at least two of four, three of five, or four of six replicate assays. (*C*, *Top*) Immunoblot for STING in HeLa-Ohio cells transduced with siRNAs targeting *STING* and paired "C911" siRNAs with complementary substitutions of nucleotides 9 to 11. PPIase B (cyclophilin B) served as a loading control. (*C*, *Bottom*) Protection against RV-A2 CPE provided by *STING*-targeting and C911 siRNAs. ***Adjusted $P = 0.0002$ by two-way ANOVA. (*D*, *Left*) Deconvolution of siRNA pool targeting STING, showing protection afforded by individual siRNAs against CPE due to RV-A2, RV-A16, or RSV. For each siRNA, $P < 0.001$ by two-way ANOVA. (*D*, *Right*) Protection against CPE due to CV-B3, with siRNA targeting PI4KB included as a positive control. ****Adjusted *P* value <0.001 by two-way ANOVA with Sidak's multiple comparison test. (*E*). *STING* mRNA and RV-A16 RNA abundance normalized to *GAPDH* mRNA in primary SAECs transduced with *STING*-targeting siRNAs. ****Adjusted *P* value < 0.001 by two-way ANOVA with Sidak's multiple comparison test. $n = 3$. (*F*) Immunofluorescence detection of RV-A16 antigen in SAECs (red). Nuclei were counterstained with DAPI (blue).

cognate RV internal ribosome entry site (IRES). These data show that STING is not required for protein translation directed by the rhinovirus IRES but instead is required for a step in the synthesis of new RV-A and RV-C RNA genomes.

Canonical STING Signaling Remains Functional in RV-A16–Infected Cells. Because our data show that STING functions as a proviral host factor during RV-A and RV-C replication, we assessed the impact of RV infection on the canonical role of STING in innate immune signaling. Although agonists activating cGAS-STING signaling induce type I IFN responses capable of suppressing RV-A replication (31), there is little evidence that RV-A infection elicits STING signaling. We found that IFN-β (*IFNB1*) mRNA responses to RV-A16 infection were closely linked to increasing STING expression in Dox-induced Huh-7/hSTING cells (Fig. 3 *A* and *B*). While the increases in *IFNB1* message were likely due to enhanced RV-A16 replication secondary to greater STING expression (Fig. 3*B*), RV-B14–induced *IFNB1* expression also correlated positively with increased STING abundance, even though increases in STING did not enhance RV-B14 replication (Fig. 3 *B* and *C*). This suggests that STING contributes directly to the IFN-β response to RV infection. Nonetheless, in RV-A16–infected HeLa cells, we did not detect any increase in the molecular size of STING that would be indicative of posttranslational modifications (e.g., phosphorylation or palmitoylation) that typically accompany STING activation (32–34) (Fig. 3*D*). Overall, RV-A16 induced substantially greater *IFNB1* responses than RV-B14, most likely because RV-B14 replicated to higher levels than RV-A16 when cells were infected at comparable multiplicities (Fig. 3 *E* and *F*). Interestingly, neither RV-A16 nor RV-B14 infection induced significant

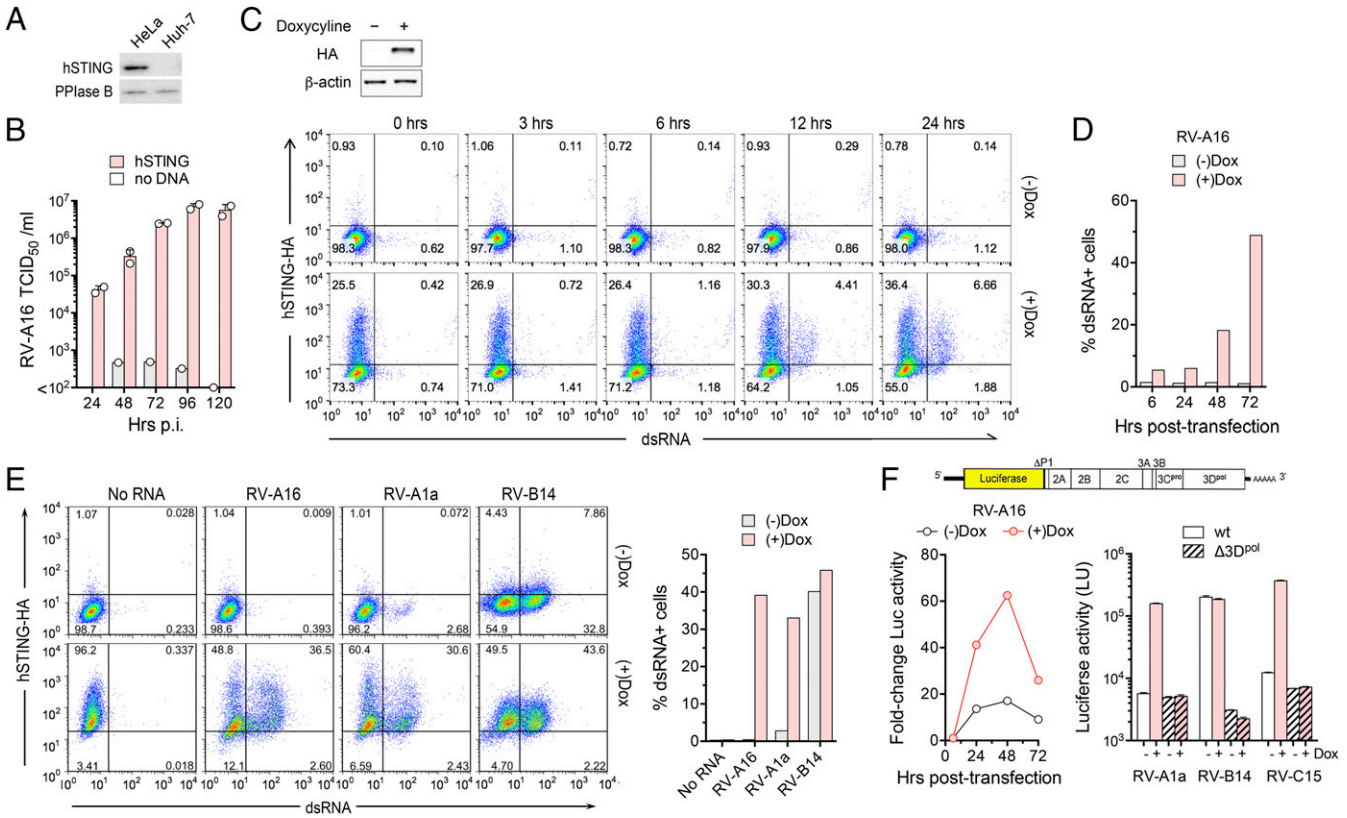

Fig. 2. STING is an essential host factor for replication of RV-A and RV-C RNA genomes. (*A*) Immunoblot of STING abundance in HeLa-Ohio and Huh-7scr cells, with PPIase B included as a loading control. (*B*) Infectious RV-A16 yield from Huh-7 cells with and without transfection of vector DNA expressing STING-HA before infection. (*C, Top*) STING-HA expression in Huh-7/hSTING cells before and after doxycycline induction. Actin was included as a loading control. (*C, Bottom*) Flow cytometry measurement of dsRNA and hSTING expression in uninduced or induced Huh-7/hSTING cells at 0 to 24 h following infection with cell-free RV-A16 virus (MOI of 3). (*D*) Proportion of all cells with dsRNA signals above threshold following transfection of synthetic RV-A16 RNA (*SI Appendix*, Fig. S3*A*). (*E, Left*) Flow cytometry of Huh-7/hSTING cells at 24 h following transfection with RV-A16, RV-A1a, or RV-B14 RNA under (–)Dox (uninduced) or (+)Dox (induced) conditions. Cells were labeled with antibodies to STING-HA and dsRNA. (*E, Right*) Proportion of all cells with dsRNA signals above threshold. (*F, Top*) Structure of subgenomic luciferase-expressing RV-A1a replicon RNA lacking a P1 (capsid-encoding) sequence. (*F, Bottom Left*) Luciferase expression following transfection of induced (+)Dox or noninduced (–)Dox Huh-7/hSTING cells with RV-A16 replicon RNAs. (*F, Bottom Right*) Luciferase expression at 18 h after transfection of induced and noninduced Huh-7/hSTING cells with RV-A1a, RV-B14, and RV-C15 replicon RNAs with or without replication-lethal mutations in the $3D^{pol}$ polymerase.

expression of the IRF3-dependent, IFN-stimulated gene *IFIT1* (Fig. 3*E*). This suggests that the impact of STING on *IFNB1* transcription may be largely driven by NF-κB activation under these conditions.

Transfection of STING agonists cGAMP or immunostimulatory DNA (ISD) into cells infected with either RV-A16 or RV-B14 led to posttranslational modification and degradation of STING, suggesting that cGAS-STING signaling remained largely intact (Fig. 3*D*). ISD-induced STING modifications were reduced in HeLa cells infected with RV-A16 compared with RV-B14–infected or uninfected cells, however, suggesting that RV-A16 might sequester STING, partially impairing signaling. Despite this, there was no reduction in *IFNB1* or *IFIT1* responses to either cGAMP or ISD in RV-A16–infected cells (Fig. 3*E*). Infection with either virus led to small decreases in the *IFNB1* and *IFIT1* responses to transfected poly(I:C), which is sensed by the RIG-I–like helicase MDA5 that signals through a STING-independent pathway. Overall, the differences in cGAMP- and ISD-induced STING signaling in infected and uninfected cells were minimal.

Canonical STING Activation Is Not Required for RV-A16 Host Factor Activity. Under basal conditions, STING is expressed as an inactive loose dimer on membranes of the ER (35, 36). When activated by binding cyclic dinucleotide GMP-AMP (cGAMP), STING forms polymers and traffics to the ER-Golgi intermediate compartment (ERGIC) and Golgi, where it is palmitoylated and phosphorylated by TANK-binding kinase 1 (TBK1) (32–34). We considered the possibility that RV-A16 might usurp step(s) in STING activation to mobilize membranes from the ER to promote the assembly of replication organelles; however, as noted above, infection with RV-A16 did not induce either posttranslational modification or degradation of STING (Fig. 3*D*). RNAi-mediated depletion of Sar1, a small GTPase that regulates the ER-to-Golgi translocation of STING (37), caused an approximate 10-fold reduction in RV-A16 RNA replication (*SI Appendix*, Fig. S6*A*). However, Sar1 depletion similarly impacted RV-B14 replication, suggesting that the effect resulted from a global defect in vesicle trafficking, not from impaired STING activation. As a further indication that STING activation is not required for RV-A16 replication, Cys-to-Ser substitutions at Cys88 and Cys91, sites of palmitoylation in STING, did not reduce the ability of ectopically expressed STING to promote replication in Huh-7 cells (*SI Appendix*, Fig. S6*B*). In contrast, an additional Ser substitution at Cys64, which is within the critical second transmembrane domain of STING and not palmitoylated, ablated RV-A16 host factor activity (*SI Appendix*, Fig. S6*B*).

Chemical inhibitors of STING palmitoylation, 2-bromopalmitate (2-BP) and H-151 (33), also failed to inhibit RV-A16 infection (*SI Appendix*, Fig. S6 *C* and *D*). Finally, in contrast to the Cys64/88/91Ser mutant, an hSTING mutant lacking the C-terminal tail (CTT),

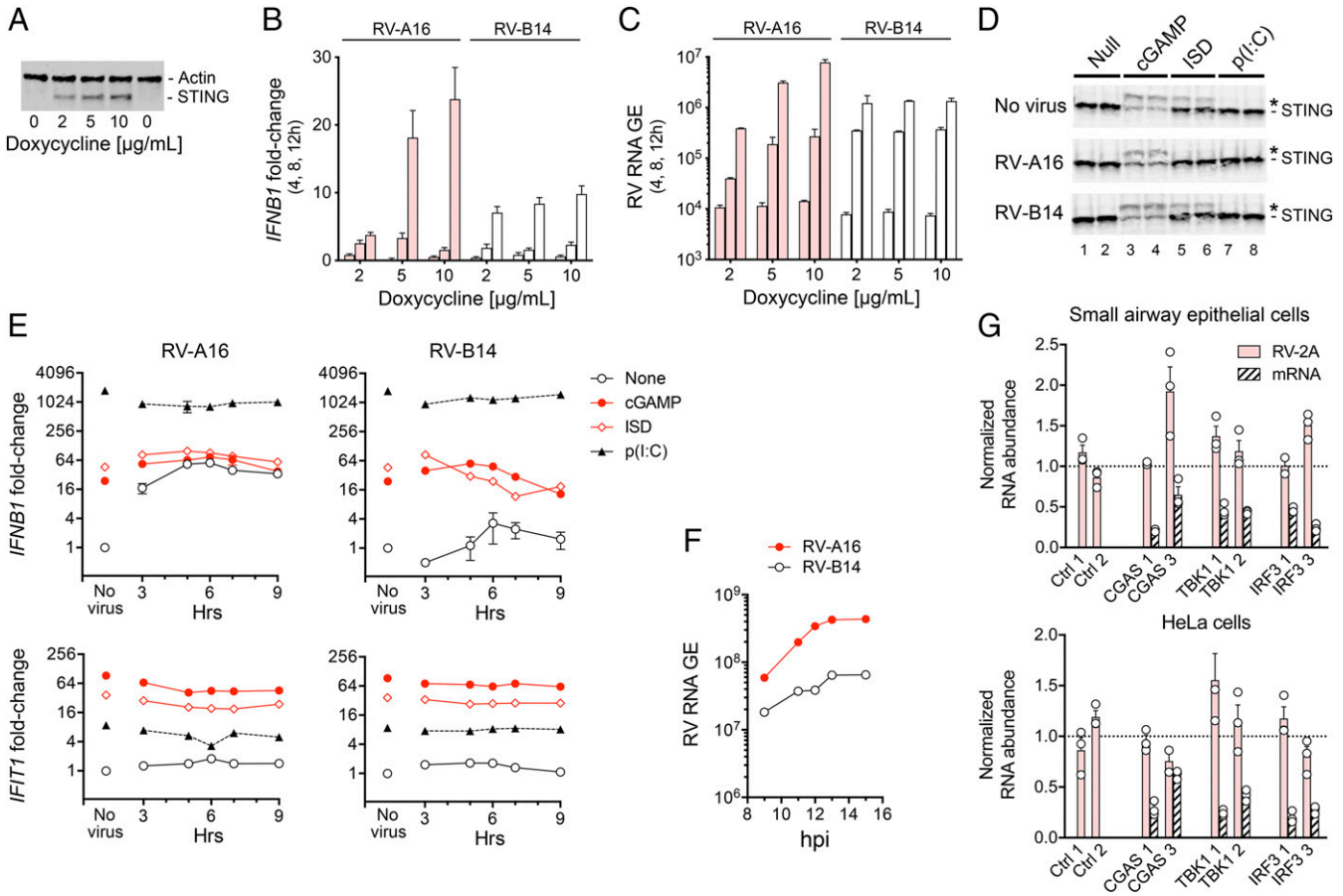

Fig. 3. IFN and STING signaling in rhinovirus-infected cells. (*A*) Immunoblot showing variable expression of STING in Huh-7/hSTING cells induced by treatment for 3 d with the indicated concentrations of doxycycline. (*B*) IFN-β (*IFNB1*) mRNA levels induced by RV-A16 and RV-B14 in Huh-7/hSTING cells at 4, 8, and 12 h postinfection (MOI of 3). Cells were induced with different concentrations of doxycycline as in *A*. Doxycycline-related increases in RV-B14–induced IFN-β mRNA were statistically significant ($P = 0.0002$ by two-way ANOVA). (*C*) RV-A16 and RV-B14 RNA abundance in Huh-7/hSTING cells at 4, 8, and 12 h under the conditions shown in *B*. (*D*) Immunoblots for STING in lysates of HeLa-H1 cells either mock-infected or infected with RV-A16 or RV-B14 and then exposed to the innate immune agonists cGAMP, ISD, or poly(I:C). Slowly migrating STING species (*) are phosphorylated or have otherwise been modified post-translationally. (*E*) HeLa cells were transfected with cGAMP, ISD, poly-(I:C), or no agonist ("none") between 3 and 9 h following infection, as indicated, with RV-A16 (*Left*) or RV-B14 (*Right*). Cells were harvested, and *IFNB1* (*Top*) and *IFIT1* (*Bottom*) mRNAs were quantified 6 h after transfection of the agonists. *IFNB1* and *IFIT1* responses in uninfected cells are shown at the left of each graph. (*F*) Viral RNA abundance in infected cells treated with no agonist in *E*. (*G*) RT-qPCR quantitation of RV-A2 and host cell target mRNAs in (*Top*) primary human SAECs or (*Bottom*) HeLa cells transfected with siRNAs targeting *CGAS*, *TBK1*, or *IRF3*. Data shown represent differences in abundance relative to mean abundance in cells transfected with nontargeting siRNAs (Ctrl 1 and Ctrl 2).

which undergoes phosphorylation by TBK1 during STING activation and mediates IRF3 signaling, retained substantial RV-A16 host factor activity (*SI Appendix*, Fig. S6*B*). This indicates that phosphorylation of STING and subsequent IRF3 activation are not required to support RV-A16 replication. Consistent with this, RNAi-mediated depletion of either TBK1 or IRF3, which lie downstream of STING in the cGAS-STING signaling pathway, or of cGAS itself had no impact on RV-A2 replication in either primary human SAECs or HeLa cells (Fig. 3*G*). Collectively, these data show that canonical activation of STING is not required for replication of RV-A16. STING can activate a noncanonical autophagy response independent of its signaling capacity (38, 39), but we found that the autophagy inhibitor 3-MA and the autophagy inducer Torin1 had no effect on RV-A16 replication (*SI Appendix*, Fig. S6*E*). These data are consistent with previous reports indicating that RV-A1 replication is not dependent on autophagic signaling and argue against an autophagy-related mechanism for STING support of RV-A replication (21).

RV-A Host Factor Activity of STING Is Species-Specific and Maps Genetically to the 2C Protein. Unlike human STING-HA, conditional expression of HA-tagged murine STING (Huh-7/mSTING cells) resulted in little to no increase in dsRNA replicative intermediates in RV-A16–infected cells, revealing STING host factor activity to be species-specific (Fig. 4*A*). RVs have a narrow natural host species range, but RV-A16 has been adapted to growth in mouse L cells expressing its human receptor protein, intercellular adhesion molecule 1 (ICAM1) (40). The mouse-adapted phenotype of this virus, RV-A16L, was found to map to two amino acid substitutions in the 2C protein, $Met^{121}Val$ and $Asp^{266}Asn$ (40). Unlike RV-A16, RV-A16L produced abundant dsRNA replicative intermediates in Dox-induced Huh-7/mSTING cells (Fig. 4*B*). Low levels of RV-A16L dsRNA in the absence of induction were likely due to leaky expression of mSTING below the limits of detection by immunoblotting and flow cytometry, as the adapted virus proved highly responsive to mSTING abundance. Yields of infectious RV-A16L virus were increased 100-fold in cells induced to express mSTING, whereas increases in RV-A16 yields averaged <10-fold (Fig. 4*C*). The mouse-adapted RV-A16L virus was also somewhat more responsive than its RV-A16 parent to conditional expression of human hSTING in multiple experiments, although the difference was not statistically significant. mSTING responsiveness mapped

specifically to the Met[121]Val and Asp[266]Asn mutations in the 2C protein (Fig. 4*D*). A subgenomic RNA replicon derived from RV-A16L containing these mutations also replicated robustly in Dox-induced mSTING cells (Fig. 4*E*). Collectively, these data provide a genetic link between STING host factor activity and the 2C protein, which is known to play a crucial role in the remodeling of intracellular membranes required for the assembly of replication organelles (13).

To determine which domains of the murine STING protein are functionally unable to support RV-A16 replication, we ectopically expressed a set of murine-human STING chimeras in Huh-7 cells (Fig. 4*F*). RV-A16 host factor activity mapped most strongly to the cytoplasmic ligand-binding domain (LBD), as replacing the hSTING LBD with the mSTING LBD resulted in a >98% reduction in virus yield. Swapping the transmembrane domains had a lesser impact, while the species origin of the CTT was irrelevant (Fig. 4*F*). Thus, the hSTING LBD is essential for its proviral RV-A host factor activity.

RV-A16 Replication Organelles Are Enriched in STING. Consistent with the lack of STING activation in RV-A16–infected cells, superresolution Airyscan fluorescence imaging did not reveal STING clustering suggestive of polymer formation (Fig. 5 *A*–*D*). Nonetheless, 3D reconstructions of z-stack Airyscan images revealed abundant STING in membranes in close proximity to dsRNA replication intermediates in both HeLa cells and human bronchial epithelial BEAS-2B cells (*SI Appendix*, Figs. S7*A* and S8). PI4P-enriched membrane domains colocalized with STING in both uninfected HeLa and Dox-induced Huh-7/hSTING cells, and this colocalization persisted in infected cells with increased PI4P abundance (Fig. 5 *B* and *C*, *SI Appendix*, Figs. S7*C* and S9, and Movies S1 and S2). In general, PI4P colocalized with STING to a greater extent than dsRNA (*SI Appendix*, Figs. S7 *B* and *D* and S8*B*); however, STING-specific fluorescence signals were present within organelles rich in PI4P or containing dsRNA in all three cell types. In contrast, only a small percentage of the STING fluorescent signal colocalized with either dsRNA or PI4P (*SI Appendix*, Figs. S7 *B* and *D* and S8*B*). These microscopic data suggest that the membranes of RV-A16 replication organelles contain substantial amounts of STING. However, STING was similarly present in replication organelles of cells infected with

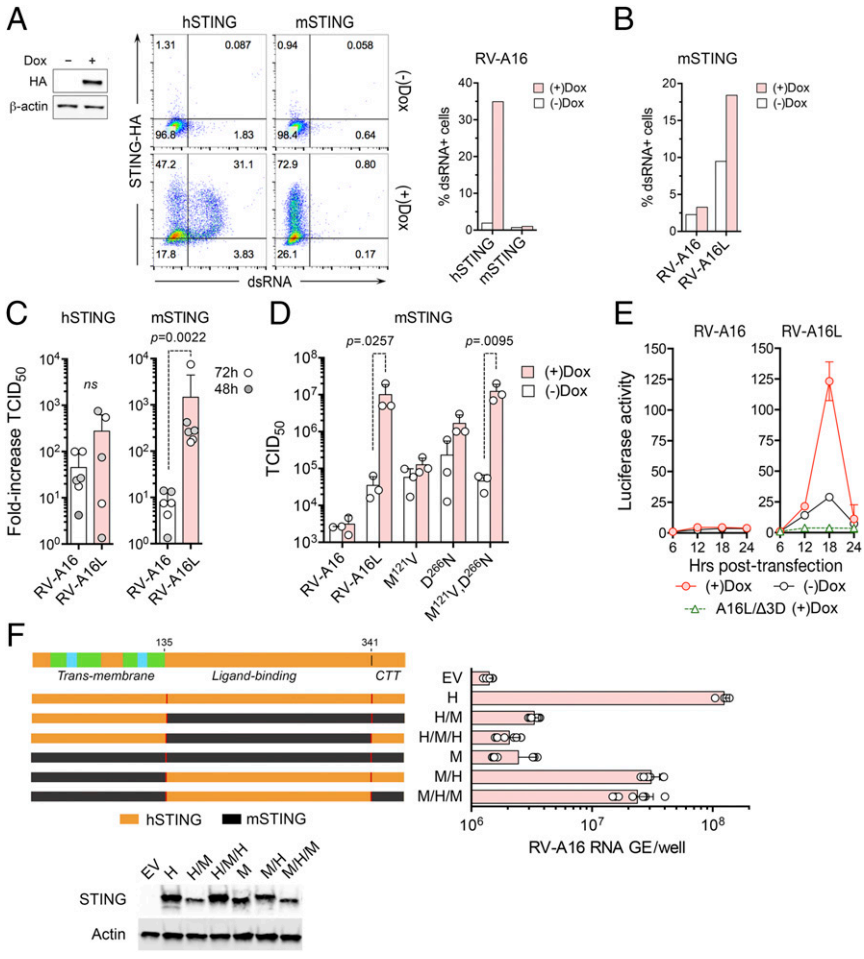

Fig. 4. Host species restriction and STING domains involved in STING utilization by RV-A16 virus. (*A*, *Left*) Immunoblot showing mSTING expression in (–)Dox and (+)Dox Huh-7/mSTING cells. (*A*, *Middle*) Flow cytometry detection of HA-tagged hSTING or mSTING and dsRNA viral replicative intermediates at 72 h after infection of (–)Dox or (+)Dox Huh-7/hSTING or Huh-7/mSTING cells with RV-A16 at an MOI of 0.1. (*A*, *Right*) Proportion of all cells with detectable dsRNA. (*B*) Levels of dsRNA viral replicative intermediates detected in cells at 72 h after infection of (–)Dox or (+)Dox Huh-7/mSTING cells with RV-A16 or RV-A16L virus. (*C*) Mean ± SD fold increase in infectious RV-A16 and RV-A16L virus yields at 48 to 72 h in (–)Dox or (+)Dox Huh-7/hSTING or Huh-7/mSTING cells. $n = 5$ or 6. (*D*) Mean ± SD infectious virus yields from (–)Dox or (+)Dox Huh-7/mSTING cells transfected with RV-A16, RV-A16L, and RV-A16 2C mutant viral RNAs (40). (*E*) Luciferase expression in (–)Dox or (+)Dox Huh-7/mSTING cells transfected with RV-A16, RV-A16L, or replication-incompetent RV-A16L/Δ3D replicon RNAs. (*F*, *Left*) Human/murine STING chimeras expressed in Huh-7 cells. Expression levels are shown in the immunoblot below. (*F*, *Right*) RV-A16 virus yields determined by RT-qPCR at 2 d after infection of transfected Huh-7 cells with RV-A16 virus at an MOI of 0.2. GE, RNA genome equivalent.

RV-B14 that has little or no requirement for STING for replication (*SI Appendix*, Fig. S7*C*).

Immunoblotting confirmed the presence of STING in RV-A16 replication organelles isolated from cytoplasmic extracts of infected cells by centrifugation in 8 to 40% buoyant density iodixanol gradients (Fig. 5 *E* and *F*). Membranes containing RV-A16 RNA banded at a density of ~1.09 g/cm^3, cofractionating with 2C and 2BC proteins and, to a lesser extent, PI4Kβ (Fig. 5 *F* and *G*). These replication organelle-containing fractions were strongly enriched for STING (Fig. 5*G*). STING was similarly present in gradient fractions containing PI4Kβ-rich membranes from RV-B14–infected cells (no antibodies to RV-B14 proteins were available). Nonetheless, in three independent experiments, STING was significantly more abundant relative to PI4Kβ in replication organelles from RV-A16–infected vs. RV-B14–infected cells (Fig. 5*H*). We sought evidence for a direct interaction between STING and RV-A16 2C protein but observed no detectable coimmunoprecipitation using either anti-2C or anti-HA antibody. We conclude that STING is present in the membranes of both RV-A16 and RV-B14 replication organelles but is particularly enriched in RV-A16 replication organelles.

Discussion

We show here that STING, an important mediator of innate immune responses to DNA virus infection, has a surprising and crucial role in replication of RV-A and RV-C rhinoviruses. This requirement exists in a variety of cell types, including primary human SAECs, and for multiple RV-A serotypes, those classified in both major and minor groups based on receptor utilization (*SI Appendix*, Fig. S4). Experiments with subgenomic replicons indicate that STING is essential for some step in the intracellular replication of the RNA genomes of RV-A and RV-C viruses (Fig. 2*F*). This requirement maps genetically to the 2C protein of RV-A16, as mouse-adaptive mutations in the 2C protein of RV-A16L allow murine STING to support replication while also enhancing the utilization of human STING (Fig. 4 *C* and *D*). Experiments in cells expressing mouse-human STING chimeras support a critical role for the cytoplasmic LBD domain of STING in defining the species-specificity of the STING host factor activity, even though the LBD domains of mouse and human STING are more closely related to each other than the transmembrane domains are (80% vs. 56% amino acid identity) (Fig. 4*F*). Despite the genetic evidence for involvement of the RV-A 2C protein, multiple attempts to demonstrate coimmunoprecipitation of 2C with STING were unsuccessful.

Under basal conditions, STING is expressed within membranes of the ER. On binding of cGAMP produced by the DNA sensor cGAS, it is mobilized from the ER to the ERGIC and ultimately to the Golgi and post-Golgi compartments (32–34). This ER-to-Golgi translocation of STING is integral to its action as an innate immune signaling mediator and is associated with phosphorylation at its C terminus by TBK1 and by its palmitoylation at Cys88 and Cys91 within the Golgi. Multiple experimental approaches demonstrated that these canonical features of STING activation are not required for RV-A replication (Fig. 3*D* and *SI Appendix*, Fig. S6); nonetheless, we suspect that some component of the activation pathway is usurped by RV-A to mobilize PI4P-enriched membranes from the ER for the assembly of replication organelles. Superresolution microscopy demonstrated substantial colocalization of PI4P with STING and, to a lesser extent, colocalization of dsRNA replication intermediates with STING in infected cells (*SI Appendix*, Figs. S7–S9). This is consistent with the relative enrichment of STING that we noted in replication organelles isolated from RV-A16–infected cells in buoyant density gradients (Fig. 5 *G* and *H*). The mechanism by which STING is mobilized from the ER to the Golgi on binding of cGAMP by the LBD domain is not well understood, and we speculate that the 2C protein usurps at least part of this mechanism to trigger the mobilization of STING and associated membranes for the assembly of RV-A replication organelles.

Given the important role of STING as a mediator of both antiviral and proinflammatory responses to virus infection, it is intriguing to consider the pathogenic consequences of STING's RV-A and RV-C host factor activity. RV-A and RV-C species viruses are generally more prevalent than RV-B (41, 42). Together they are responsible for the more severe clinical manifestations of rhinovirus disease (12), although RV-C is linked to more severe respiratory disease than RV-A (11). STING is also relatively highly expressed in lung tissue and thus may contribute to protection against both viral and bacterial respiratory tract infections (43–45). We found only minimal perturbations of STING signaling in response to cGAMP and ISD agonists in RV-A16–infected cells, and little evidence to support that this virus–host interaction alters the capacity of STING to function in innate immunity. Unfortunately, no small animal model of RV infection exists to allow assessment of the pathogenic consequences of STING utilization by RV-A and RV-C infections in vivo. Nonetheless, our data provide insight into the role of STING in host species restriction of RV infections, adding to what is already known about receptor restrictions, and may facilitate the ultimate development of animal models in which RV pathogenesis can be studied.

Methods

Cells. Huh-7 human carcinoma hepatoma cells, HeLa-H1, and HeLa-Ohio cells were cultured in DMEM supplemented with 10% FBS unless noted otherwise. Huh7scr cells were obtained from Frank Chisari, Scripps, La Jolla, CA. Human bronchial epithelial BEAS-2B cells were obtained from American Type Culture Collection (ATCC) and cultured in BEGM media (Clonetics, CC-3170). Primary SAECs were obtained from Lonza Bioscience and expanded. One donor was used for all experiments. Huh-7/hSTING and Huh-7/mSTING cell lines were derived from Huh-7 cells by transduction with lentivirus vectors expressing doxycycline-inducible hSTING or mSTING, each with a C-terminal HA tag, constructed from pCW57.1 (Addgene, 41393, a gift from David Root, Broad Institute, Cambridge, MA) and STING expression vectors provided by Scott Pesiridis, GlaxoSmithKline, Collegeville, PA (*SI Appendix, Supplementary Methods*). To induce STING, doxycycline (Sigma-Aldrich, D3447), 10 μg/mL unless specified otherwise, was added to cell cultures 24 to 36 h before infection or transfection and maintained for the duration of the experiment.

Viruses and Plasmids. Infectious molecular cDNA clones for RV-A16 and RV-B14 were a gift from Wai-Ming Lee, University of Wisconsin–Madison, Madison, WI, and clones for RV-A16L and related mutants (MV, DN, and MVDN) were provided by Vincent Racaniello, Columbia University, New York, NY. The infectious molecular clone for RV-A1a was a gift from Dan Pevear, ViroPharma, Exton, PA. A plasmid containing genome-length cDNA of the EV-D68 strain US/MO/14-18947, modified to incorporate a nanoluciferase reporter sequence upstream of VP4, was provided by Raul Andino, University of California, San Francisco, CA, and Craig Cameron, The University of North Carolina at Chapel Hill, Chapel Hill, NC. Viruses not recovered from infectious clones were purchased from ATCC. Construction of luciferase replicons for RV-A16, RV-B14, and RV-A1a has been described previously (46, 47). An infectious cDNA clone of RV-C15 and a related nanoluciferase-expressing replicon were constructed using standard methods. pcDNA3 (Thermo Fisher Scientific) and pUNO1-hSTING and pUNO1-mSTING (InvivoGen) were obtained from commercial sources. All plasmid manipulations were done using standard methods. Mutations of plasmid sequences were done by swapping in commercially purchased synthetic DNA fragments (Genewiz). Either electroporation (48) or Lipofectamine 2000 (Thermo Fisher Scientific) was used for transfection of plasmid DNAs into cells.

Antibodies and Chemical Reagents. The following antibodies were used in this study: anti–β-actin (A2228, Sigma-Aldrich); anti-HA (3724, Cell Signaling Technology, for immunoblots; 11867423001, Roche, for microscopy); anti-dsRNA (J2, SCICONS); anti-PI4P (Z-P004, Echelon Biosciences); anti-VP2 (18758, QED Bioscience); anti-RV16 2C, a gift from Roberto Solari, Imperial College, London, UK; anti-PI4Kβ (06-578, EMD Millipore); anti-STING (19851-1-AP, Proteintech and 13647, Cell Signaling Technology), anti-Sar1 (ab125871,

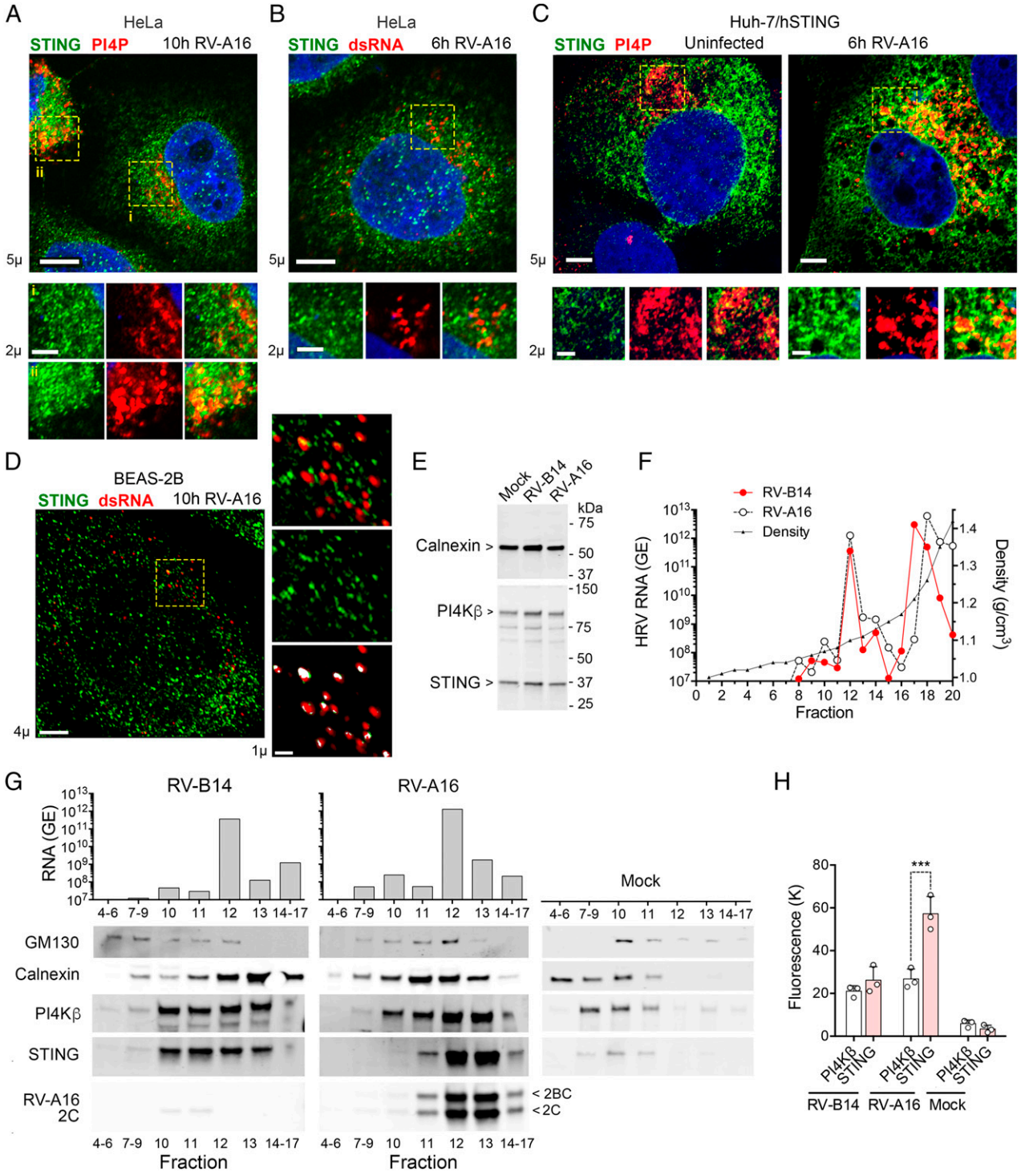

Fig. 5. Membranes of RV-A16 replication organelles are enriched for STING. (*A* and *B*) Merged superresolution Airyscan fluorescence microscopic images showing endogenous STING (green) and dsRNA (red) (*A*) or PI4P (red) (*B*) in RV-A16–infected HeLa-H1 cells at 6 to 10 h postinfection as indicated. (*C*) Airyscan images showing STING (HA; green) and PI4P (red) staining of (+)Dox Huh-7/hSTING cells before (*Left*) and 6 h after (*Right*) infection with RV-A16. Nuclei are stained with DAPI in *A*–*C*. Enlarged single-channel images of the areas bounded by yellow lines are shown at the bottom of each panel. (*D*) Airyscan superresolution image of a human bronchial epithelial BEAS-2B cell at 10 h postinfection with RV-A16 showing endogenous STING (green) and dsRNA (red). Expanded views on the right show STING and dsRNA (*Top*), STING only (*Middle*), and dsRNA (*Bottom*) with colocalizing STING voxels (white). (*E*) Immunoblot showing PI4Kβ and STING and the ER marker calnexin in unfractionated lysates of cell cultures used for isolation of RV-A16 and RV-B14 replication organelles. (*F*) RV-A16 and RV-B14 RNA abundance in fractions of buoyant density iodixanol gradients. Membrane-associated replication organelles banded at a density of ∼1.10 g/cm^3. (*G*) Immunoblots showing PI4Kβ, STING, and RV-A16 2C and 2BC along with ER (calnexin) and Golgi (GM130) markers in fractions from gradients loaded with lysates of RV-B14, RV-A16, and mock-infected HeLa-H1 cells. (*H*) Relative intensities of PI4Kβ and STING bands in immunoblots of peak gradient fractions containing replication organelles from RV-B14– and RV-A16–infected cells in three independent experiments. Protein bands visualized with infrared fluorescent secondary antibodies were quantified on an Odyssey scanner (LI-COR Biosciences). ***P = 0.0064 by unpaired t test without assuming equal SD by Holm–Sidak correction for multiple comparisons.

Abcam), and anti-cyclophilin b (PPIB; ab16045, Abcam). For flow cytometry, Pacific Blue goat anti-rabbit IgG, Alexa Fluor 647 goat anti-mouse IgG2a, and Alexa Fluor 488 goat anti-mouse IgG2b (all from Thermo Fisher Scientific) were used as secondary antibodies. In general, all antibodies were used at the manufacturer's recommended dilution. 3-MA (Sigma-Aldrich, SAE0107) was prepared as a stock solution in 2-(*N*-morpholino)ethanesulfonic acid hydrate buffer provided by the supplier. Torin1 was obtained from Tocris Biosciences.

Flow Cytometry. Cells from a 35-cm^2 dish were trypsinized and pelleted. The collected cells were first fixed in 2% paraformaldehyde and then permeabilized in 0.2% Triton X-100. Cells were then incubated with primary antibodies, followed by secondary antibodies, in 100-μL solutions containing 3% BSA, 1× PBS, and 0.1% Tween-20. After each incubation, cells were washed twice in wash buffer (1× PBS and 0.1% Tween-20). After the final wash, cells were resuspended in 500 μL of wash buffer and filtered through a FACS tube strainer cap (Corning, 352235). The resulting cells were analyzed using a Beckman Coulter CyAn ADP high-performance flow cytometer and Summit version 4.4 software.

Airyscan Superresolution Microscopy. Cells (4×10^5) were seeded onto coverslips in 24-well dishes and cultured for 24 h before rhinovirus infection. Cells were fixed with 4% paraformaldehyde for 20 min, followed by permeabilization with 0.05% saponin and blocking with 5% normal goat serum. Cells were stained for 1 to 2 h at room temperature with antibodies diluted in 0.05% saponin with 3% BSA and then mounted using ProLong Gold (Life Technologies). Imaging data were recorded in superresolution mode on a Zeiss 880 laser-scanning confocal microscope (Carl Zeiss) equipped with an Airyscan detector and Plan-Apochromat 63×/1.40 oil DIC M27 objective. For each image, fluorescence signals were recorded sequentially at different wavelengths using appropriate laser excitation and emission filter sets. The pixel size was 0.043 μm in the *x* and *y* directions and 0.160 μm in the *z* direction. The 3D reconstructions, volume rendering, and image analysis were done with Imaris 9.5 software (Bitplane).

Buoyant Density Gradient Analysis of RV Replication Organelles. HeLa cell cytoplasmic extracts were prepared as described previously at 24 h after infection at a multiplicity of infection (MOI) of 3 (49). Here 500 μL of extract (from ~10^6 cells) was layered onto iodixanol gradients prepared and subjected to ultracentrifugation as described previously (50). Fractions (250 μL) were collected from the top of the gradient. RNA for RT-qPCR was isolated from fractions using the QIAamp Viral RNA Mini Kit (Qiagen). For immunoblotting and to remove iodixanol, aliquots of fractions were diluted 1:10 in PBS and then subjected to desalting and concentration (Pierce, 88152) before being loaded onto sodium dodecyl sulfate polyacrylamide gel electrophoresis gels.

Additional details on the experimental procedures are provided in *SI Appendix*.

Data Availability. All study data are included in the main text and *SI Appendix*.

ACKNOWLEDGMENTS. We thank Vincent Racaniello for his gift of RV-A16L and related mutant cDNA plasmids; Roberto Solari for his gift of anti-2C antibody; Raul Andino and Craig Cameron for the EV-D68 plasmid; and Scott Pesiridis for hSTING and mSTING expression vectors. We also thank former members of the GlaxoSmithKline team, Jill Walker, Chris Moore, Michael Thomson, Margaret Gartland, Jeffrey Pouliot, and Tim Sheahan, for their support. This work was supported in part by grants from the National Institute of Allergy and Infectious Diseases (R01-AI103083 and R01-AI150095, to S.M.L.) and the National Center for Advancing Translational Sciences, NIH (KL2TR002490, to K.V.S.).

1. S. E. Jacobs, D. M. Lamson, K. St George, T. J. Walsh, Human rhinoviruses. *Clin. Microbiol. Rev.* **26**, 135–162 (2013).
2. A. C. Palmenberg *et al*., Sequencing and analyses of all known human rhinovirus genomes reveal structure and evolution. *Science* **324**, 55–59 (2009).
3. M. Calışkan *et al*., Rhinovirus wheezing illness and genetic risk of childhood-onset asthma. *N. Engl. J. Med.* **368**, 1398–1407 (2013).
4. F. D. Martinez, Childhood asthma inception and progression: Role of microbial exposures, susceptibility to viruses and early allergic sensitization. *Immunol. Allergy Clin. North Am.* **39**, 141–150 (2019).
5. C. J. Britto, V. Brady, S. Lee, C. S. Dela Cruz, Respiratory viral infections in chronic lung diseases. *Clin. Chest Med.* **38**, 87–96 (2017).
6. C. K. Kim, Z. Callaway, J. E. Gern, Viral infections and associated factors that promote acute exacerbations of asthma. *Allergy Asthma Immunol. Res.* **10**, 12–17 (2018).
7. A. C. Palmenberg, J. E. Gern, Classification and evolution of human rhinoviruses. *Methods Mol. Biol.* **1221**, 1–10 (2015).
8. Y. A. Bochkov *et al*., Cadherin-related family member 3, a childhood asthma susceptibility gene product, mediates rhinovirus C binding and replication. *Proc. Natl. Acad. Sci. U.S.A.* **112**, 5485–5490 (2015).
9. M. K. Iwane *et al*., Human rhinovirus species associated with hospitalizations for acute respiratory illness in young US children. *J. Infect. Dis.* **204**, 1702–1710 (2011).
10. E. Bergroth *et al*., Rhinovirus type in severe bronchiolitis and the development of asthma. *J. Allergy Clin. Immunol. Pract.* **8**, 588–595.e4 (2020).
11. J. Bizzintino *et al*., Association between human rhinovirus C and severity of acute asthma in children. *Eur. Respir. J.* **37**, 1037–1042 (2011).
12. N. Khetsuriani *et al*., Novel human rhinoviruses and exacerbation of asthma in children. *Emerg. Infect. Dis.* **14**, 1793–1796 (2008).
13. N. Y. Hsu *et al*., Viral reorganization of the secretory pathway generates distinct organelles for RNA replication. *Cell* **141**, 799–811 (2010).
14. K. Bienz, D. Egger, L. Pasamontes, Association of polioviral proteins of the P2 genomic region with the viral replication complex and virus-induced membrane synthesis as visualized by electron microscopic immunocytochemistry and autoradiography. *Virology* **160**, 220–226 (1987).
15. I. Romero-Brey, R. Bartenschlager, Endoplasmic reticulum: The favorite intracellular niche for viral replication and assembly. *Viruses* **8**, 160 (2016).
16. C. E. Melia *et al*., Origins of enterovirus replication organelles established by whole-cell electron microscopy. *MBio* **10**, e00951-19 (2019).
17. H. Lyoo *et al*., ACBD3 is an essential pan-enterovirus host factor that mediates the interaction between viral 3A protein and cellular protein PI4KB. *MBio* **10**, e02742-18 (2019).
18. P. S. Roulin *et al*., Rhinovirus uses a phosphatidylinositol 4-phosphate/cholesterol counter-current for the formation of replication compartments at the ER-Golgi interface. *Cell Host Microbe* **16**, 677–690 (2014).
19. E. Abernathy *et al*., Differential and convergent utilization of autophagy components by positive-strand RNA viruses. *PLoS Biol.* **17**, e2006926 (2019).
20. W. T. Jackson *et al*., Subversion of cellular autophagosomal machinery by RNA viruses. *PLoS Biol.* **3**, e156 (2005).
21. K. A. Klein, W. T. Jackson, Human rhinovirus 2 induces the autophagic pathway and replicates more efficiently in autophagic cells. *J. Virol.* **85**, 9651–9654 (2011).
22. M. Brabec-Zaruba, U. Berka, D. Blaas, R. Fuchs, Induction of autophagy does not affect human rhinovirus type 2 production. *J. Virol.* **81**, 10815–10817 (2007).
23. A. Ablasser, Z. J. Chen, cGAS in action: Expanding roles in immunity and inflammation. *Science* **363**, eaat8657 (2019).
24. H. Ishikawa, G. N. Barber, STING is an endoplasmic reticulum adaptor that facilitates innate immune signalling. *Nature* **455**, 674–678 (2008).
25. L. Jin *et al*., MPYS, a novel membrane tetraspanner, is associated with major histocompatibility complex class II and mediates transduction of apoptotic signals. *Mol. Cell. Biol.* **28**, 5014–5026 (2008).
26. B. Zhong *et al*., The adaptor protein MITA links virus-sensing receptors to IRF3 transcription factor activation. *Immunity* **29**, 538–550 (2008).
27. W. Sun *et al*., ERIS, an endoplasmic reticulum IFN stimulator, activates innate immune signaling through dimerization. *Proc. Natl. Acad. Sci. U.S.A.* **106**, 8653–8658 (2009).
28. E. Buehler, Y. C. Chen, S. Martin, C911: A bench-level control for sequence specific siRNA off-target effects. *PLoS One* **7**, e51942 (2012).
29. H. Ishikawa, Z. Ma, G. N. Barber, STING regulates intracellular DNA-mediated, type I interferon-dependent innate immunity. *Nature* **461**, 788–792 (2009).
30. Y. Zhang *et al*., Structural and virological studies of the stages of virus replication that are affected by antirhinovirus compounds. *J. Virol.* **78**, 11061–11069 (2004).
31. G. Pépin *et al*., Activation of cGAS-dependent antiviral responses by DNA intercalating agents. *Nucleic Acids Res.* **45**, 198–205 (2017).
32. S. L. Ergun, D. Fernandez, T. M. Weiss, L. Li, STING polymer structure reveals mechanisms for activation, hyperactivation, and inhibition. *Cell* **178**, 290–301.e10 (2019).
33. S. M. Haag *et al*., Targeting STING with covalent small-molecule inhibitors. *Nature* **559**, 269–273 (2018).
34. T. Saitoh *et al*., Atg9a controls dsDNA-driven dynamic translocation of STING and the innate immune response. *Proc. Natl. Acad. Sci. U.S.A.* **106**, 20842–20846 (2009).
35. L. Sun, J. Wu, F. Du, X. Chen, Z. J. Chen, Cyclic GMP-AMP synthase is a cytosolic DNA sensor that activates the type I interferon pathway. *Science* **339**, 786–791 (2013).
36. A. Ablasser *et al*., cGAS produces a 2′–5′-linked cyclic dinucleotide second messenger that activates STING. *Nature* **498**, 380–384 (2013).
37. E. Ogawa, K. Mukai, K. Saito, H. Arai, T. Taguchi, The binding of TBK1 to STING requires exocytic membrane traffic from the ER. *Biochem. Biophys. Res. Commun.* **503**, 138–145 (2018).
38. D. Liu *et al*., STING directly activates autophagy to tune the innate immune response. *Cell Death Differ.* **26**, 1735–1749 (2019).

39. X. Gui *et al*., Autophagy induction via STING trafficking is a primordial function of the cGAS pathway. *Nature* **567**, 262–266 (2019).
40. J. R. Harris, V. R. Racaniello, Changes in rhinovirus protein 2C allow efficient replication in mouse cells. *J. Virol.* **77**, 4773–4780 (2003).
41. W. M. Lee *et al*., Human rhinovirus species and season of infection determine illness severity. *Am. J. Respir. Crit. Care Med.* **186**, 886–891 (2012).
42. J. E. Linder *et al*., Human rhinovirus C: Age, season, and lower respiratory illness over the past 3 decades. *J. Allergy Clin. Immunol.* **131**, 69–77.e6 (2013).
43. E. Lam, S. Stein, E. Falck-Pedersen, Adenovirus detection by the cGAS/STING/TBK1 DNA sensing cascade. *J. Virol.* **88**, 974–981 (2014).
44. M. Uhlén *et al*., Proteomics. Tissue-based map of the human proteome. *Science* **347**, 1260419 (2015).
45. J. S. Ruiz-Moreno *et al*.; CAPNETZ Study Group, The common HAQ STING variant impairs cGAS-dependent antibacterial responses and is associated with susceptibility to Legionnaires' disease in humans. *PLoS Pathog.* **14**, e1006829 (2018).
46. K. L. McKnight, S. M. Lemon, Capsid coding sequence is required for efficient replication of human rhinovirus 14 RNA. *J. Virol.* **70**, 1941–1952 (1996).
47. K. L. McKnight, The human rhinovirus internal cis-acting replication element (cre) exhibits disparate properties among serotypes. *Arch. Virol.* **148**, 2397–2418 (2003).
48. D. Yamane *et al*., Differential hepatitis C virus RNA target site selection and host factor activities of naturally occurring miR-122 3′ variants. *Nucleic Acids Res.* **45**, 4743–4755 (2017).
49. K. Bienz, D. Egger, Y. Rasser, W. Bossart, Intracellular distribution of poliovirus proteins and the induction of virus-specific cytoplasmic structures. *Virology* **131**, 39–48 (1983).
50. Z. Feng *et al*., A pathogenic picornavirus acquires an envelope by hijacking cellular membranes. *Nature* **496**, 367–371 (2013).